Stochastic behavior of the coefficient of normal restitution

Nina Gunkelmann, Marina Montaine, and Thorsten Pöschel
Institute for Multiscale Simulations, Friedrich-Alexander-Universität, Erlangen, Germany
(Received 6 December 2013; published 28 February 2014)

We consider the collision of a rough sphere with a plane by detailed analysis of the collision geometry. Using stochastic methods, the effective coefficient of restitution may be described as a fluctuating quantity whose probability density follows an asymmetric Laplace distribution. This result agrees with recent experiments by Montaine *et al.* [Phys. Rev. E **84**, 041306 (2011)].

DOI: 10.1103/PhysRevE.89.022205 PACS number(s): 45.70.−n, 61.72.Lk, 61.50.Ks, 64.70.Nd

I. INTRODUCTION

The dynamics of rapid granular flows and granular gases is governed by dissipative collisional interactions of particles with each other and with the system walls. Assuming instantaneous interaction, for smooth particles the dissipative character of particle interactions may be quantified by the coefficient of normal restitution (COR), $\varepsilon < 1$, defined as

$$\varepsilon = -\frac{\vec{V}\,' \cdot \vec{n}}{\vec{V} \cdot \vec{n}}\,, \tag{1}$$

where $\vec{V}$ and $\vec{V}\,'$ are the relative velocities of the colliding particles before and after the collision, and $\vec{n}$ is the unit vector normal to the impact plane in the instant of the collision.

The COR is the most important characteristic of a granular system leading to many exciting effects such as characteristic velocity correlations [1,2], violation of molecular chaos [3], non-Maxwellian velocity distribution [4,5], overpopulated high-energy tails of the distribution function [6], anomalous diffusion and other transport coefficients [7–9], cluster instabilities [10,11], and many others; see, e.g., [12]. In virtually all publications on granular gases and rapid granular flows, it is assumed that the COR is either a constant or a function of the impact velocity. This is in contrast to several experimental results, e.g., [13–18], where it was found that even for almost spherical particles, the COR reveals significant scatter, which cannot be explained by the imperfections of the experiment but must be attributed to tiny imperfections of the surfaces in contact. Performing large-scale bouncing ball experiments using a robot, Montaine *et al.* [19] analyzed the fluctuations of the COR of more than 10^5 single impacts and found that besides the known dependence on impact velocity, the COR may be described as a fluctuating quantity whose probability distribution is a combination of two exponentials,

$$p_\varepsilon(t) = \begin{cases} be^{at}, & t < \varepsilon_{\max}, \\ de^{-ct} & \text{otherwise}, \end{cases} \tag{2}$$

where a, b, c, d, and $\varepsilon_{\max}$ are parameters depending on the impact velocity. Besides being of interest *per se*, the knowledge of the functional form of the distribution function may be of importance also for the theory of granular gases, since recent theoretical and numerical work shows that the assumption of a fluctuating COR leads to measurable and nontrivial hydrodynamics effects in granular systems [20].

So far, the distribution Eq. (2) is a purely empirical result, based only on experimental data. However, there is a lack of theoretical interpretation of this exceptional probability distribution. The aim of the present paper is to derive the distribution $p(\varepsilon)$ by analyzing the geometry of the impact in detail. To this end, in Sec. II we relate the (global) coefficient of restitution, which describes the dynamics of a particle to the local impact properties for a given collision geometry, quantified by the *contact vector*. The stochastic properties of the contact vector are computed in Sec. III, and in Sec. IV we combine both ingredients to obtain finally the distribution function of the coefficient of restitution, ε.

II. GLOBAL VERSUS LOCAL COEFFICIENT OF RESTITUTION

We consider a rigid particle consisting of a large central sphere of radius ϱ and mass M which is covered by a large number, $N \gg 1$, of tiny asperities at uniformly distributed random positions on its surface [19]. Each of the asperities is represented by a sphere of radius $\rho \ll \varrho$ and mass m. It is further assumed that the coverage of the surface of the central sphere is sufficiently dense such that each contact of the particle with a plane occurs through one of the asperities. For typical values $\rho/\varrho \lesssim 10^{-4}$, thus $m/M \lesssim 10^{-12}$ and $N \sim 10^6$, we can safely neglect the contribution of the asperities to the mass and the moment of inertia of the particle. For the subsequent analysis, we chose the coordinate system with the origin located at the center of the central sphere and the x-y plane being in parallel to the plate.

The particle is dropped from a certain height and collides with a horizontal hard plate. We describe the inelastic collision of the particle with the plate as an instantaneous event leading to a change of linear and angular momentum of the particle due to the collisional impulse $\vec{P}$:

$$\begin{aligned} \Delta\vec{V} &\equiv \vec{V}\,' - \vec{V} = \frac{1}{M}\vec{P}, \\ \Delta\vec{\Omega} &\equiv \vec{\Omega}\,' - \vec{\Omega} = \frac{1}{J}(\vec{r} \times \vec{P}), \end{aligned} \tag{3}$$

where $\vec{V}$ and $\vec{V}\,'$ describe the pre- and postcollisional linear velocity of the particle, $\vec{\Omega}$ and $\vec{\Omega}\,'$ are the pre- and postcollisional angular velocities, J is the moment of inertia of the particle, and $\vec{r}$ is the contact point, located at the surface of

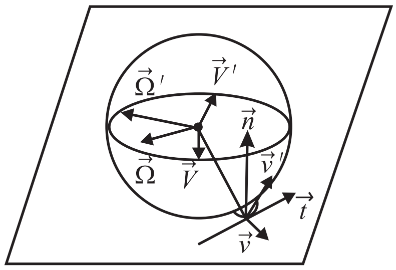

FIG. 1. Sketch of the collision of a rough particle with a flat surface. Only the asperity which is in contact with the plane is shown.

one of the asperities. The geometry of the impact is sketched in Fig. 1.

The *microscopic* impact velocity, that is, the velocity of the point where the asperity touches the floor at $\vec{r}$, is defined by

$$\vec{v} = (\vec{v}\cdot\vec{n})\vec{n} + (\vec{v}\cdot\vec{t})\vec{t} = \vec{V} + \vec{\Omega}\times\vec{r}\,, \tag{4}$$

where $\vec{n}$ and $\vec{t}$ are unit vectors in the plane pointing in directions normal and tangential to the velocity of the contact point.

The inelastic nature of the collision of the particle with the plate is taken into account by the *microscopic* coefficients of normal and tangential restitution, ϵ_n and ϵ_t, such that the postcollisional velocity at the point of contact is given by

$$\begin{aligned}\vec{v}\,'\cdot\vec{n} &= -\epsilon_n(\vec{v}\cdot\vec{n}),\\ \vec{v}\,'\cdot\vec{t} &= \epsilon_t(\vec{v}\cdot\vec{t}).\end{aligned} \tag{5}$$

The third component of $\vec{v}$ which is perpendicular to both $\vec{n}$ and $\vec{t}$ does not change during the impact.

The change of the *microscopic* impact velocity of the particle is, therefore,

$$\begin{aligned}\vec{v}\,' - \vec{v} &= -(1+\epsilon_n)(\vec{v}\cdot\vec{n})\vec{n} + (-1+\epsilon_t)(\vec{v}\cdot\vec{t})\vec{t}\\ &= \Delta\vec{V} + \Delta\vec{\Omega}\times\vec{r}.\end{aligned} \tag{6}$$

The second line of Eq. (6) relates the change of the microscopic velocity at the point of contact to the change of the macroscopic velocities of the particle. By substituting $\Delta\vec{V}$ and $\Delta\vec{\Omega}$ from Eq. (3) into the right-hand side of Eq. (6), we obtain the following system of linear equations describing the impact:

$$\begin{aligned}&-(1+\epsilon_n)(\vec{v}\cdot\vec{n})\vec{n} + (-1+\epsilon_t)(\vec{v}\cdot\vec{t})\vec{t}\\ &\quad = \frac{\vec{P}}{M} + \frac{1}{J}(\vec{r}\times\vec{P})\times\vec{r}.\end{aligned} \tag{7}$$

Using Eqs. (7) and (3), one can compute the dynamics of the bouncing particle provided the position of the asperity $\vec{r}_c$ and the *local* coefficients of restitution, ϵ_n and ϵ_t, are given. Consequently, by means of Eq. (1), we can compute the *macroscopic* coefficient of restitution, ε, as observed in experiments. Obviously, as the position of the asperity at the instant of the impact is random, $\vec{v}$ and thus ε are fluctuating quantities, too. Consequently, the stochastic properties of the coefficient of normal restitution, ε, are intimately related to the distribution of the asperities at the surface of the particle.

While *a priori* we do not know the value of ε, for a concrete geometry at impact the value of the microscopic coefficient of restitution is less problematic: Assuming viscoelastic material

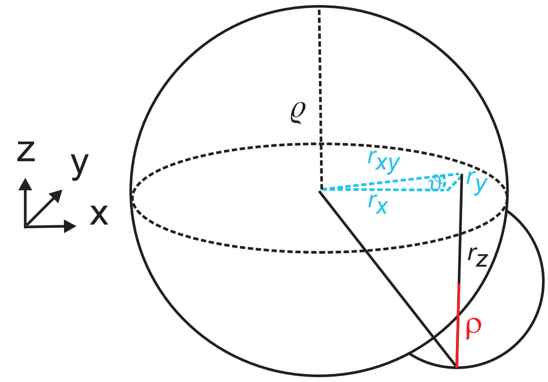

FIG. 2. (Color online) Definition of the variables describing the impact geometry.

properties, the coefficient of restitution of a smooth body impacting a plane is given by [21–23]

$$\epsilon_n(v) = 1 + \sum_{i=0}^{\infty} h_i \alpha^{\frac{i}{2}} v^{\frac{i}{10}}, \tag{8}$$

where h_i are analytically known, universal (material-independent) constants, and α is a function of particle mass, size, and material properties (see [23] for the numerical values of h_i and α). Even though Eq. (8) is analytically known, any truncation of the infinite sum in Eq. (8) leads to divergence, $\epsilon_n \to \pm\infty$, therefore, for practical reasons, here we prefer the convergent Padé expansion of Eq. (8) of order [1/4] [24,25]:

$$\epsilon_n(v) \approx \frac{1 + c_1 v_*}{1 + b_1 v_* + b_2 v_*^2 + b_3 v_*^3 + b_4 v_*^4}, \quad v_* = \beta^{1/2} v^{1/10} \tag{9}$$

with the universal constants $c_1 = 0.501\,086$, $b_1 = 0.501\,086$, $b_2 = 1.153\,45$, $b_3 = 0.577\,977$, and $b_4 = 0.532\,178$. The material constant $\beta = 0.0467$ was used, corresponding to the experimental values by Montaine *et al.* [19] for the collision of stainless-steel spheres. This approximation assures the correct limit, $\lim_{v\to\infty}\epsilon_n(v) = 0$.

The *microscopic* coefficient of tangential restitution, ϵ_t, depends on both bulk material properties and surface properties. Therefore, ϵ_t cannot be analytically derived from material properties, except for the limiting case of pure Coulomb friction, e.g., [26,27]. Here we assume $\epsilon_t = 1$, that is, elastic no-slip interaction in the tangential direction.

III. DISTRIBUTION OF THE CONTACT VECTOR $\vec{r}$

A. Components of the contact vector

To compute the stochastic properties of the coefficient of normal restitution, ε, through Eqs. (7), (3), and (1), we consider the statistical distribution of the vector $\vec{r}$ indicating the point where the particle contacts the plane through one of its asperities; see Fig. 1. From geometry it is clear that the contacting asperity is the one which is closest to the south pole of the large central sphere; see Fig. 2.

Due to the random orientation of the particle and the random distribution of the asperities on its surface, the components of $\vec{r} = (r_x, r_y, r_z)$ obey probability densities which will be computed in this section. The components r_x and r_y can be expressed by the length of the projection of $\vec{r}$ to the plane, $r_{xy} \equiv \sqrt{r_x^2 + r_y^2}$, and the angle ϑ (see Fig. 2) such that

$$r_x = r_{xy} \cos\vartheta, \quad r_y = r_{xy} \sin\vartheta. \tag{10}$$

The remaining coordinate, r_z, follows from r_{xy} via

$$r_z = -\sqrt{\varrho^2 - r_{xy}^2} - \rho. \tag{11}$$

In the following subsections, we compute the probability densities of r_{xy}, $\cos\vartheta$, and $\sin\vartheta$ and derive then the probability densities of the components of $\vec{r}$.

B. Probability density of r_{xy}

The probability of finding k homogeneously distributed asperities in a small circle of area A obeys a binomial distribution which for $N \gg 1$ may be approximated by a Poisson distribution

$$p_k(A) = \frac{e^{-\lambda A}(\lambda A)^k}{k!}, \tag{12}$$

where $\lambda = N/(4\pi\varrho^2)$ follows from equating the total number of asperities N on the surface of the central sphere with the expectation value of k due to $p_k(4\pi\varrho^2)$. We specify A as the area of a circle with radius r_{xy}; see Fig. 2. Note that for computing λ we approximated the area of the cap of the sphere by the area of a flat circle of the same radius. For the numerical values of $N = 10^5$ and $\varrho = 3 \times 10^{-3}$ m, the resulting error is negligible. We obtain the cumulative probability, $P_{r_{xy}}$, to find at least one asperity in a circle of radius r_{xy},

$$P_{r_{xy}}(t) = 1 - \exp(-\lambda\pi t^2), \quad t \geqslant 0 \tag{13}$$

and by differentiating we obtain the probability density for the distance of the closest asperity to the south pole:

$$p_{r_{xy}}(t) = 2\pi t\lambda \exp(-\lambda\pi t^2), \quad t \geqslant 0. \tag{14}$$

Note that the probability for a direct contact of the central sphere with the plane is negligibly small. It corresponds to the probability of finding no asperity in a circle of radius R_* around the south pole with $(\varrho + \rho)^2 = R_*^2 + (\varrho - \rho)^2$, that is, $R_* = 2\sqrt{\varrho\rho} \approx 7 \times 10^{-4}$ m. According to Eqs. (12) and (13), this probability is $\exp(-\lambda\pi R_*^2) \approx 10^{-106}$, which means that the corresponding event is extremely unlikely to occur.

C. Angular location of the contact point in the plane

Given the particle contacts the plane at the distance r_{xy} from the z axis, the possible locations of the contact point are on a circle of radius r_{xy} where no angular orientation, ϑ, is preferred. Thus, the angle is homogeneously distributed in the interval $\vartheta \in [0,2\pi)$. Consequently, the cumulative probabilities of $\sin\vartheta$ and $\cos\vartheta$ read

$$\begin{aligned} P_{\cos\vartheta}(t) &\equiv P(\cos\vartheta \leqslant t) \\ &= 1 - [P(\vartheta \in [0, \arccos t]) \\ &\quad + P(\vartheta \in [2\pi - \arccos t, 2\pi])] \\ &= 1 - \frac{1}{\pi}\arccos t, \end{aligned} \tag{15}$$

$$\begin{aligned} P_{\sin\vartheta}(t) &\equiv P(\sin\vartheta \leqslant t) \\ &= \begin{cases} 1 - P(\vartheta \in [\arcsin t, \pi - \arcsin t]) & \text{if} \quad t \geqslant 0 \\ 1 - [P(\vartheta \in [0, \pi - \arcsin t]) & \\ +P(\vartheta \in [2\pi + \arcsin t, 2\pi])] & \text{if} \quad t < 0 \end{cases} \\ &= 1 - \frac{1}{\pi}\arccos(t). \end{aligned} \tag{16}$$

Differentiating Eqs. (15) and (16), we obtain the probability densities

$$\begin{aligned} p_{\cos\vartheta}(t) &= \frac{1}{\pi}\frac{1}{\sqrt{1-t^2}}, \\ p_{\sin\vartheta}(t) &= \frac{1}{\pi}\frac{1}{\sqrt{1-t^2}}. \end{aligned} \tag{17}$$

D. Joint probability distribution for the components of the contact point

According to Eq. (10), the components of $\vec{r}$ are products of r_{xy} and $\cos\vartheta$ or $\sin\vartheta$, respectively. Since the distributions of r_{xy} and ϑ (and thus $\cos\vartheta$ and $\sin\vartheta$) are statistically independent [28], we obtain the distribution of the product via

$$\begin{aligned} p_{r_x}(t) &= p_{r_y}(t) = p_{r_{xy}\cos\vartheta}(t) = p_{r_{xy}\sin\vartheta}(t) \\ &= \int_{-\infty}^{\infty} \frac{1}{|q|} p_{\cos\vartheta}(q)\, p_{r_{xy}}\left(\frac{t}{q}\right) dq \\ &= \begin{cases} \int_{-1}^{1} \frac{\frac{2t}{q}\pi\lambda \exp\left[-\lambda\pi\left(\frac{t}{q}\right)^2\right]}{\sqrt{1-q^2}} \frac{1}{|q|\pi}\, dq & \text{for} \quad \frac{t}{q} \geqslant 0 \\ 0 & \text{otherwise} \end{cases} \\ &= \begin{cases} \int_{-1}^{0} -\frac{\frac{2t}{q^2}\lambda \exp\left[-\lambda\pi\left(\frac{t}{q}\right)^2\right]}{\sqrt{1-q^2}}\, dq & \text{for} \quad t \leqslant 0 \\ \int_{0}^{1} \frac{\frac{2t}{q^2}\lambda \exp\left[-\lambda\pi\left(\frac{t}{q}\right)^2\right]}{\sqrt{1-q^2}}\, dq & \text{for } t > 0 \end{cases} \\ &= \sqrt{\lambda}e^{-\pi\lambda t^2}. \end{aligned} \tag{18}$$

We see that the probability density distribution for r_x and r_y is a normal distribution. Our main assumption is the modeling of the particle's surface by an ideal central sphere overimposed by a large number of *identical* and *semispherical* microscopic impurities. Both assumptions are essential for the analytical calculations. Whereas we do not believe that the concrete shape of the microscopic asperities is of importance, we are aware that for more realistic modeling the asperities should vary in size, possibly in a hierarchical way. Micromechanically, different sizes would lead to modifications of the contact geometry. In particular, smaller asperities would be screened by larger ones, which leads, effectively, to a reduction of the density of the asperities since not all of them can come into contact with the plane. While this reduction may lead to quantitative changes, for the functional form of the distribution of the coefficient of restitution it would be essential that the distribution p_{r_x} is Gaussian, which was checked by means of simulations.

To verify the obtained distribution functions for the components of the contact vector, Eq. (18), we performed a simulation of an elastic particle covered by $N = 10^5$, $\varrho = 3 \times 10^{-3}$ m,

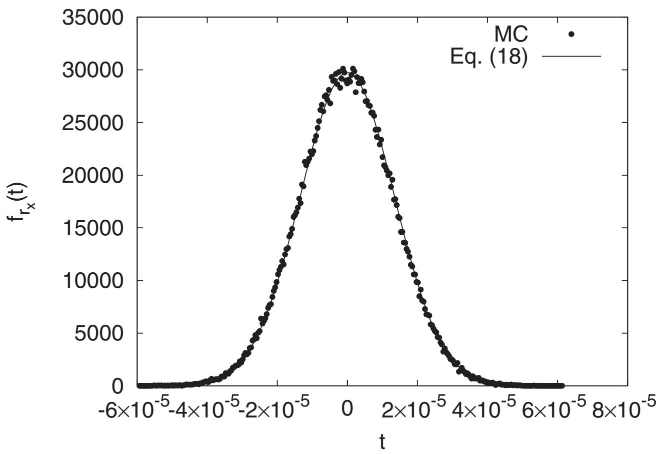

FIG. 3. Histograms of the x and y components of the contact vector as found in numerical simulations together with the corresponding analytical results for the density distributions due to Eq. (18).

and $\rho = 6.5 \times 10^{-7}$ m. The particle was released at random orientation and the statistics of the components of the contact vector were recorded. The numerical and analytical results are compared in Fig. 3.

IV. DISTRIBUTION OF THE COEFFICIENT OF NORMAL RESTITUTION

To obtain the distribution of the coefficient of normal restitution, we use Eq. (3) together with the definition Eq. (1),

$$\varepsilon = -1 - \frac{1}{M}\frac{\vec{P}\cdot\vec{n}}{\vec{V}\cdot\vec{n}}. \tag{19}$$

The impulse $\vec{P}$ is found by solving the system Eq. (7):

$$\vec{P} = -K(\vec{V},\vec{\Omega},\vec{r})M\begin{pmatrix} r_x r_z \\ r_y r_z \\ I + r_z^2 \end{pmatrix} \tag{20}$$

with

$$K(\vec{V},\vec{\Omega},\vec{r}) \equiv [1+\epsilon_n(v)]\frac{(\vec{V}\cdot\vec{n} + \Omega_x r_y - \Omega_y r_x)}{\vec{r}^{\,2} + I} \tag{21}$$

with the components of the precollisional angular velocity $\vec{\Omega} = (\Omega_x,\Omega_y,\Omega_z)$ and the velocity at the contact point in the z direction, $V = (\vec{V} + \vec{\Omega}\times\vec{r})\cdot\vec{n}$ and $I \equiv J/M$. Inserting in Eq. (19) yields

$$\varepsilon = -1 + \frac{K(\vec{V},\vec{\Omega},\vec{r})\left(I + r_z^2\right)}{\vec{V}\cdot\vec{n}} \tag{22}$$

The moment of inertia of the particle is

$$J = \frac{2}{5}M\varrho^2. \tag{23}$$

The solution of Eq. (7) for the postcollisional angular velocity reads

$$\vec{\Omega}' = \vec{\Omega} + K(\vec{V},\vec{\Omega},\vec{r})\begin{pmatrix} r_y \\ -r_x \\ 0 \end{pmatrix}. \tag{24}$$

The postcollisional linear velocity reads

$$\vec{V}' = \vec{V} - K(\vec{V},\vec{\Omega},\vec{r})\begin{pmatrix} r_x r_z \\ r_y r_z \\ I + r_z^2 \end{pmatrix}. \tag{25}$$

For the computation of ε according to Eq. (1), only the orientation of the z axis of the coordinate system is important. The orientation of the y and z axes in the plane is arbitrary and can be chosen for each collision such that $\Omega_x = -\Omega_y$, which simplifies Eq. (21). The fluctuating quantity $r_x r_y$ has mean zero and a very small variance, which suggests the approximation $r_x + r_y \approx (r_x^2 + r_y^2)^{1/2} = r_{xy}$, whose distribution is known, Eq. (14). Then Eq. (21) adopts the form

$$K(\vec{V},\vec{\Omega},\vec{r}) \equiv [1+\epsilon_n(v)]\frac{(\vec{V}\cdot\vec{n} + \Omega_x r_{xy})}{\vec{r}^{\,2} + I} \tag{26}$$

From geometry (see Fig. 2; $\varrho \gg \rho$) it is clear that r_z has a much smaller fluctuation range than r_x and r_y; therefore, r_z can be assumed constant with $r_z = \varrho + \rho$.

With these approximations, K and thus ε [Eq. (22)] contain only a single fluctuating quantity, which is r_{xy}. Hence, the distribution of $\varepsilon = g(r_{xy})$ can be calculated by the transformation

$$p_\varepsilon(t) = p_{r_{xy}}[g^{-1}(t)]\frac{dg^{-1}(t)}{dt}, \tag{27}$$

where $p_{r_{xy}}$ is the probability density function of r_{xy}. From Eqs. (22) and (26), we obtain

$$p_\varepsilon(t) = -\frac{\pi\lambda[Q\Omega_x + f(t)]Q[h(t) + f(t)\Omega_x]}{2V_z^2(1+t)^3 f(t)}\exp\left[-\frac{\pi\lambda[h+f(t)]^2}{4(1+t)^2V_z^2}\right], \tag{28}$$

$$f(t) \equiv \sqrt{[1+\epsilon_n(v)]Q\Omega_x^2 + 4V_z^2[-t^2 + t\epsilon_n(v) - t + \epsilon_n(v)]\left(I + r_z^2\right)}, \tag{29}$$

$$h(t) \equiv 2(1+t)V_z^2 + Q\Omega_x^2, \tag{30}$$

$$Q \equiv [1+\epsilon_n(v)]\left(I + r_z^2\right). \tag{31}$$

We checked the result of Eq. (28) numerically for a particular set of parameters, $V_z = v = 1.3\ \frac{\text{m}}{\text{s}}$, $\Omega_x = 0.2$, $N = 10^5$ asperities, $\varrho = 3 \times 10^{-3}$ m, and $\rho = 6.5 \times 10^{-7}$ m, and we found very good agreement; see Fig. 4. The component Ω_x'

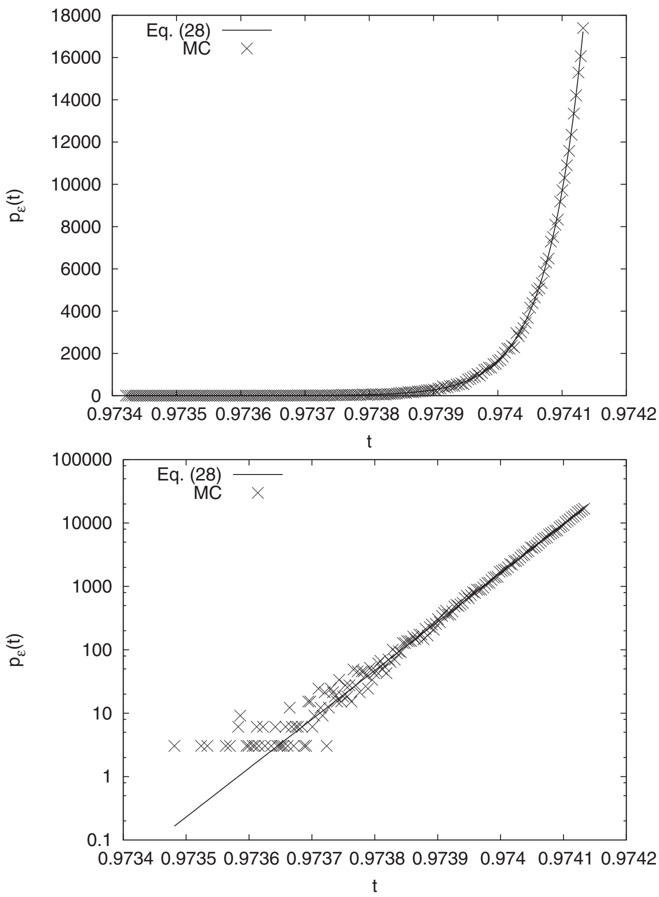

FIG. 4. Numerical test of Eq. (28) by means of Monte Carlo simulations shows almost perfect agreement for the analytical and numerical data. The lower figure shows the same data in log-scale. For details, see the text.

can be expressed in terms of r_y:

$$\Omega_x' = \Omega_x + \frac{r_z P_y - r_y P_z}{I} = \Omega_x + \frac{1}{I}\left[\frac{P_z r_z^2 r_y}{r_z^2 + I} - r_y P_z\right]. \quad (32)$$

Consequently, as r_y obeys a Gaussian distribution and r_z is approximately constant, Ω_x' is Gaussian-distributed with zero mean as well. Its standard deviation reads

$$\sigma = \frac{P_z}{I\sqrt{2\lambda\pi}}\left(1 + \frac{r_z^2}{r_z^2 + I}\right), \quad (33)$$

where $P_z = MV_z(-\varepsilon - 1)$ is the z component of the collisional impulse.

The result, Eqs. (32) and (33), was checked by means of a Monte Carlo simulation of 100 000 drops of a sphere covered by 100 000 asperities; see Fig. 5. To obtain the numerical data, we generated random values of r_y according to the probability distribution given by Eq. (18) and ε according to the probability distribution obtained via Eq. (28) and calculating 100 000 times Ω_x' for the start values $\Omega_x = 0$, $\vec{V} \cdot \vec{n} = 1$ m/s, $\varrho = 3 \times 10^{-3}$ m, and $\rho = \varrho \times 10^{-4}$ m.

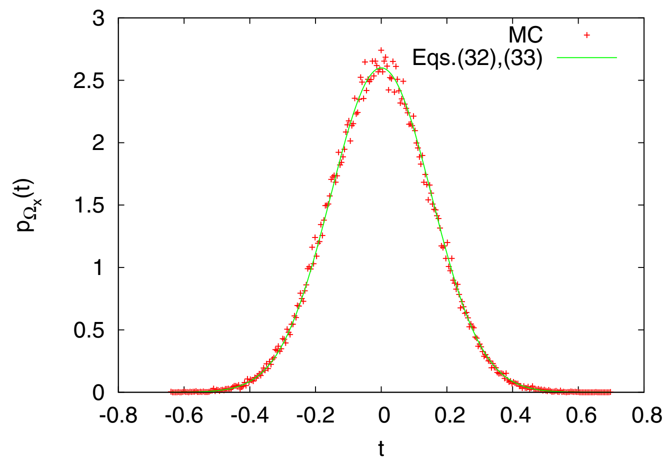

FIG. 5. (Color online) The numerical test of Eqs. (32) and (33) by means of Monte Carlo simulations shows almost perfect agreement for the analytical and numerical data. For details, see the text.

V. COEFFICIENT OF RESTITUTION FOR A ROUGH BALL: NUMERICAL TEST

In bouncing ball experiments [19], the coefficient of restitution of a rough ball was characterized as a fluctuating quantity obeying an asymmetric Laplace distribution, Eq. (2). To compare the analytical result for the probability distribution of a rough sphere, Eq. (28) with the experiment, we perform a corresponding Monte Carlo simulation using a particle of radius $\varrho = 3$ mm covered by 10^6 asperities of size $\rho = 5 \times 10^{-4}$ mm. We assume the initial velocity, $V_z = \vec{V} \cdot \vec{n} = 1$ m/s, and angular velocity, $\vec{\Omega} = \vec{0}$, and we choose ε from the analytically obtained distribution Eq. (28) to obtain V_z' via

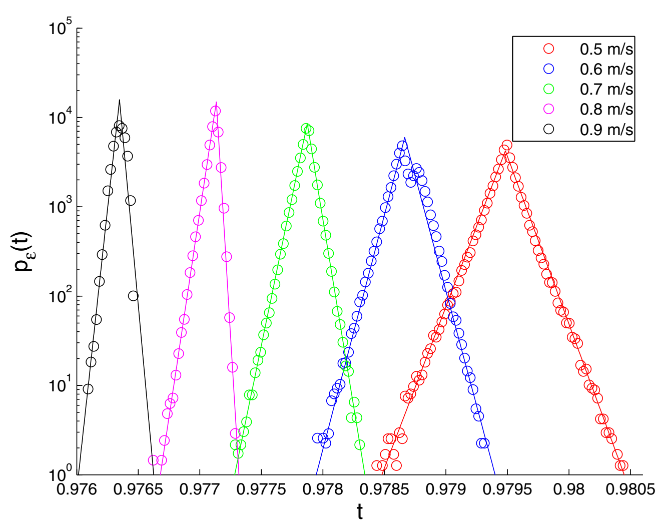

FIG. 6. (Color online) Probability density of the coefficient of restitution, ε, due to Eq. (28) for different values of the impact velocity. For the Monte Carlo simulation, we assume a particle of size $\varrho = 3$ mm covered by 10^6 asperities of size $\rho = 5 \times 10^{-4}$ mm. The distribution is approximately Laplacian (see exponential fits, full lines) and shows good agreement with the experimental data; see Fig. 4 in Ref. [19].

Eq. (1) and we randomly generate Ω_x' according to Eqs. (32) and (33) and update the impact velocity using Eq. (25). This procedure is iterated until the linear velocity decreases to 0.1 m/s. This process corresponds to the bouncing ball experiment [19]. From the statistical data obtained by repeating the process 10^5 times, we can draw the histogram for the coefficient of restitution, ε. Figure 6 shows five histograms of ε for different impact velocities. The resulting probability density is approximately an asymmetric Laplace distribution of the form Eq. (2). Comparison with Fig. 4 in Ref. [19] shows good agreement with the experimental data.

VI. CONCLUSION

The coefficient of restitution (COR) describing the dissipative interaction of granular particles is of great importance for the physics of granular matter. It is the foundation of kinetic theory of granular gases and rapid granular flows based on the Boltzmann equation, e.g., [29], and thus granular hydrodynamics, e.g., [30]. Moreover, event-driven molecular dynamics of granular systems is based on the COR. Therefore, a profound knowledge of the properties of the COR is a necessary prerequisite for the adequate description of dynamical granular systems. In virtually all publications so far, it is assumed that the COR is either a material constant or a deterministic function of the material and system characteristics and the impact velocity. This assumption is in contrast to experimental results, e.g., [13–18], which show that even tiny surface textures, that is, even weak roughness, cause significant scatter of the COR, which suggests that the COR is a fluctuating quantity. These fluctuations have been investigated in large-scale experiments [19] to obtain the probability density for the COR of almost smooth particles, which was reported to be of asymmetric Laplacian shape. Based on this experimental result, it could be shown [20] that the fluctuations of the COR have a measurable influence on the kinetic properties of granular gases.

So far, the Laplacian shape of the probability density was a conjecture based on experimental observations and computer simulations presented in [20]. Considering the statistical properties of the particle's surface at the region of contact, the present paper shows theoretically that this conjecture is justified and that the origin of the fluctuations is indeed the microscopic roughness of the surface of the particles.

ACKNOWLEDGMENTS

The authors thank the Deutsche Forschungsgemeinschaft (DFG) for funding through the Cluster of Excellence "Engineering of Advanced Materials."

[1] T. P. C. van Noije, M. H. Ernst, R. Brito, and J. A. G. Orza, Phys. Rev. Lett. **79**, 411 (1997).

[2] W. T. Kranz, N. V. Brilliantov, T. Pöschel, and A. Zippelius, Eur. Phys. J. ST **179**, 91 (2009).

[3] T. Pöschel, N. V. Brilliantov, and T. Schwager, Int. J. Mod. Phys. C **13**, 1263 (2002).

[4] G. A. and S. M., J. Fluid Mech. **282**, 75 (1995).

[5] I. Goldhirsch, S. H. Noskowicz, and O. Bar-Lev, in *Granular Gas Dynamics*, Vol. 624 of *Lecture Notes in Physics* (Springer, Berlin, 2003), p. 37.

[6] S. E. Esipov and T. Pöschel, J. Stat. Phys. **86**, 1385 (1997).

[7] N. V. Brilliantov and T. Pöschel, Chaos **15**, 026108 (2005).

[8] N. V. Brilliantov and T. Pöschel, Phys. Rev. E **61**, 1716 (2000).

[9] N. Brilliantov and T. Pöschel, Phys. Rev. E **67**, 061304 (2003).

[10] I. Goldhirsch and G. Zanetti, Phys. Rev. Lett. **70**, 1619 (1993).

[11] T. Pöschel, N. V. Brilliantov, and T. Schwager, J. Phys. Condens. Matter **17**, S2705 (2005).

[12] N. Brilliantov and T. Pöschel, *Kinetic Theory of Granular Gases* (Oxford University Press, Oxford, 2003).

[13] J. M. Lifshitz and H. Kolsky, J. Mech. Phys. Solids **12**, 35 (1964).

[14] A. P. Hatzes, F. G. Bridges, and D. N. C. Lin, Mon. Not. R. Astron. Soc. **231**, 1091 (1988).

[15] H. King, R. White, I. Maxwell, and N. Menon, Europhys. Lett. **93**, 14002 (2011).

[16] E. Falcon, C. Laroche, S. Fauve, and C. Coste, Eur. Phys. J. B **3**, 45 (1998).

[17] C. M. Sorace, M. Y. Louge, M. D. Crozier, and V. H. C. Law, Mech. Res. Commun. **36**, 364 (2009).

[18] G. McLaskey and S. Glaser, J. Acoust. Soc. Am. **128**, 1087 (2010).

[19] M. Montaine, M. Heckel, C. Kruelle, T. Schwager, and T. Pöschel, Phys. Rev. E **84**, 041306 (2011).

[20] N. Gunkelmann, D. Serero, and T. Pöschel, New J. Phys. **15**, 093030 (2013).

[21] N. V. Brilliantov, F. Spahn, J.-M. Hertzsch, and T. Pöschel, Phys. Rev. E **53**, 5382 (1996).

[22] T. Schwager and T. Pöschel, Phys. Rev. E **57**, 650 (1998).

[23] T. Schwager and T. Pöschel, Phys. Rev. E **78**, 051304 (2008).

[24] R. Ramírez, T. Pöschel, N. V. Brilliantov, and T. Schwager, Phys. Rev. E **60**, 4465 (1999).

[25] P. Müller and T. Pöschel, Phys. Rev. E **84**, 021302 (2011).

[26] T. Schwager, V. Becker, and T. Pöschel, Eur. Phys. J. E **27**, 107 (2008).

[27] V. Becker, T. Schwager, and T. Pöschel, Phys. Rev. E **77**, 011304 (2008).

[28] P. A. Lewis and G. Shedler, Nav. Res. Logist. Quart. **26**(3), 403 (1979).

[29] N. V. Brilliantov and T. Pöschel, *Kinetic Theory of Granular Gases* (Oxford University Press, Oxford, 2004).

[30] I. Goldhirsch, Annu. Rev. Fluid Mech. **35**, 267 (2003).